2012

Incorporation of the Actin-Myosin Biomolecular Motor System into a Microfluidic Device

Rebecca Marie Ragland
lilshortee135@aol.com

**INCORPORATION OF THE ACTIN-MYOSIN BIOMOLECULAR
MOTOR SYSTEM INTO A MICROFLUIDIC DEVICE**

A Thesis submitted to
the Graduate College of
Marshall University

In partial fulfillment of
the requirements for the degree of

Master of Science

Chemistry

by
Rebecca Marie Ragland

Approved by

Dr. Brian Scott Day, Committee Chairperson
Dr. Eric Blough
Dr. Leslie Frost

Marshall University
May 2012

Acknowledgments

First and foremost, I would like to thank God for putting me in the position to achieve my goals, not only in this research, but also in every other aspect of my life. To my fiancé, Dana Lycans, I love you and thank you for putting up with all of my frustrations throughout the course of this research. I also greatly appreciate my parents, Doug and Emily Ragland, for supporting me throughout my undergraduate and graduate years and helping me to achieve my goals.

Michael Tanner deserves a big acknowledgment for working with me on this research for most of my time as a graduate student. Also, Cat Higgins and Jessica Nicely provided greatly needed assistance. Rebekah Jamieson, Erik Vint, Chris Warner, Zach Hunter, and Phillip Kirk also all provided friendship and help during the time we worked in the lab together.

I would like to thank my advisor Dr. Scott Day for all of his help on this project, as well as Dr. Eric Blough, who helped to initiate this research and provided many of the materials. Special thanks also go to Dr. Leslie Frost for being a member of my committee and to Dr. Mike Norton for allowing me to use his lab space, instruments, and supplies. Dr. Kevin Rice and David Neff deserve special recognition for the time they took to teach me about various instruments and to troubleshoot problems. All of the other faculty members of the Marshall University Chemistry Department have also been very supportive during my entire collegiate career.

I would also like to acknowledge the NASA West Virginia Space Grant Consortium for the Graduate Research Fellowship that was awarded to me for this project. The financial support provided by this program allowed me to focus my attention solely on school and research.

Table of Contents

List of Figures

Abstract

Recently, the field of bionanotechnology has sought to develop a device containing a biomolecular motor nano-cargo transport system. Among many applications, a device of this sort could be used to sort, purify, or detect specific molecules. In this work, an attempt was made to incorporate the actin-myosin biomolecular motor system into a microfluidic device constructed out of polydimethylsiloxane (PDMS) and glass. Methods for cleaning and functionalizing the glass surface of the device were optimized. After performing actin-myosin motility assays in a variety of PDMS/glass devices, it was determined that the oxygen permeability of PDMS limited the quality of motility that could be obtained upon illumination. Heavy treatment (20 minutes) of the PDMS surface with an air plasma allowed for more prolonged motility. More efforts to reduce the permeability of PDMS and improve motility will have to be made before a functional device can be achieved.

Background

Biomolecular motors are enzymes that convert chemical energy into mechanical energy, typically by using adenosine triphosphate (ATP) as fuel. ATP hydrolysis is used to drive many biological processes because it is a highly exergonic reaction. There are several different biomolecular motors found in eukaryotic cells, including linear and rotary types. Myosin, kinesin, and dynein are examples of linear molecular motors, which use the energy from ATP to achieve a net displacement[1]. The main focus of this paper will be a system containing the myosin motor.

Myosins are molecular motor proteins that bind actin filaments and use ATP to fuel a conformational change, allowing actin to slide relative to the myosin. Biologically, they have a large role in muscle contraction, as well as intracellular cargo transport. There are several types of myosin; at least 18 classes were known in 2006[2]. The basic structure of myosin consists of a heavy polypeptide chain with a globular head and a tail. Often, other light chains are attached to the head. The tails of two heavy chains wrap around each other in a coil to form dimers in types such as myosin II and myosin V[2]. The process of ATP hydrolysis for most types of myosin is quite similar; however, some other features vary among the different types. Myosin II is referred to as conventional myosin and is found in skeletal, heart, and smooth muscle cells, along with nonmuscle cells[2]. The investigation of muscle myosin began in 1864[3] and still continues to this day. At physiological ionic strengths, myosin is insoluble[4]. However, using tryptic digestion, myosin can be progressively cleaved to generate fragments that are soluble. With low exposure to trypsin, myosin II can be cleaved into light meromyosin (LMM) and heavy meromyosin (HMM). HMM consists of a truncated coiled-tail portion with the two globular heads still intact (Figure 1). Further cleavage can separate the two heads from the remaining tail portion. The head

portion is referred to as subfragment-1 (S1)[2]. Both the nucleotide- and actin-binding regions are found on the myosin head, although located on opposite sides[5].
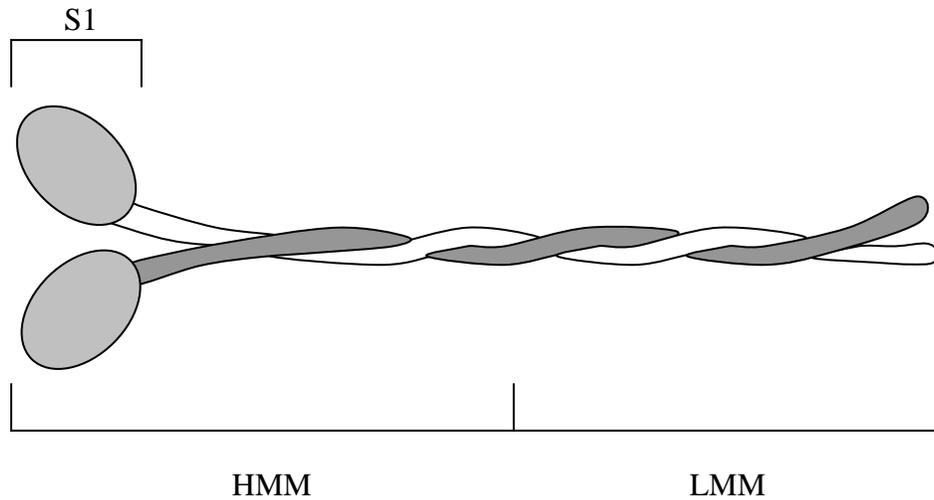
Figure 1. Schematic of a myosin II molecule.

Actin is also present in muscle fiber and is a major component of the cytoskeleton in eukaryotic cells[6]. Actin filaments (F-actin) are helically-shaped strands of G-actin (globular actin) monomers with approximately a 7 nanometer diameter (Figure 2). Each G-actin is added to the strand in the same orientation, creating polarity in the filament[2]. Under cellular conditions, G-actin and F-actin exist in similar quantities. To achieve polymerization of actin *in vitro*, physiological ionic strength conditions must be used[7]. To stabilize the filaments and guard against depolymerization, phalloidin, a toxic component of *Amanita phalloides*, is added *in vitro*[8]. Actin filaments can also be bundled *in vitro* using the bundling protein fascin.
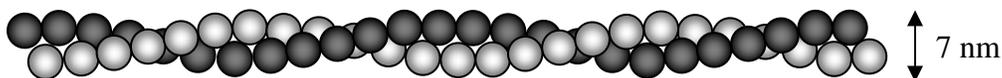
Figure 2. Schematic of an actin filament. The black and gray coloration depicts the two helical strands of G-actin monomers (represented by individual spheres) that are coiled together to form F-actin.

In 1986, Kron and Spudich developed an *in vitro* motility assay for the actin-myosin system[9]. Using fluorescence microscopy, fluorescently labelled actin filaments could be visualized moving across a glass surface coated with myosin filaments. Over time, many improvements and modifications to the assay have been made. Myosin fragments such as HMM are frequently used in *in vitro* motility assays now (see Figure 3). Actin bundles made using fascin have been shown to exhibit the same sliding velocity *in vitro* as actin filaments, while providing greater rigidity[10]. It has also become standard for the glass surface to be coated with nitrocellulose prior to HMM binding to enhance motility. However, trimethylchlorosilane (TMCS)-derivatized glass surfaces have been shown to support actin-myosin motility as well or better than the standard nitrocellulose surfaces[11]. Figure 4 shows the reaction of TMCS with free hydroxyl groups on a clean glass surface, which creates trimethylsilyl groups. These groups are thought to promote the adsorption of HMM molecules in orientations that support motility[12].
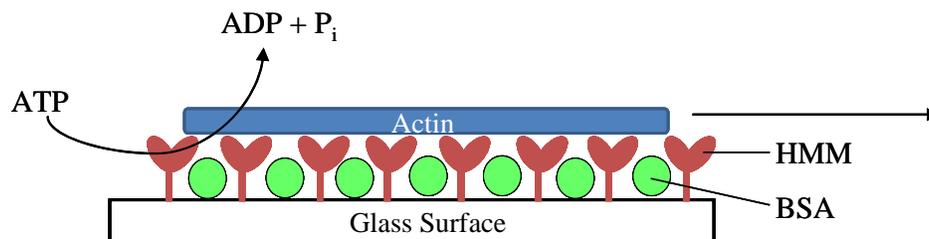
Figure 3. Schematic of an actin-myosin *in vitro* motility assay. HMM molecules are attached to a modified glass surface (nitrocellulose-coated or functionalized with trimethylsilyl groups). The remaining glass surface is blocked with bovine serum albumin (BSA) before the addition of actin. When ATP is introduced, it is hydrolyzed by the myosin heads, resulting in a conformational change which propels the actin forward.

(CH₃)₃ (CH₃)₃ (CH₃)₃ (CH₃)₃

$(CH_3)_3$ $(CH_3)_3$ $(CH_3)_3$ $(CH_3)_3$

Si   Si   Si   Si

O   O   O   O

Si   Si   Si   Si

TMS-Functionalized Glass

OH   OH   OH   OH

Si   Si   Si   Si

Clean Glass

$+\ H_3C-Si-CH_3$ with CH_3 above and Cl below $\longrightarrow$
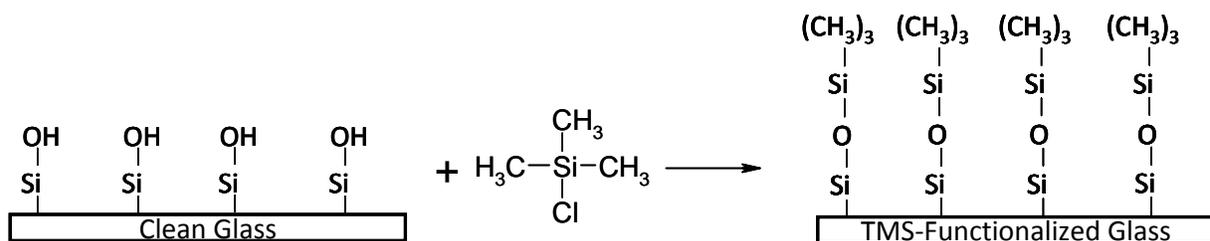
Figure 4. Reaction of TMCS with hydroxyl groups on a glass surface to produce a surface functionalized with trimethylsilyl (TMS) groups.

Introduction

Due to the ease with which motility can be achieved *in vitro* using biomolecular motors, there has been much interest during recent years in incorporating these motors into the growing field of nanotechnology for cargo transport applications. In order to facilitate any type of transport system, including those on the molecular level, several essential components are required. In this case, myosin or kinesin molecules function as the motor and ATP is the fuel source. It is also necessary to have a "road" or guide for direction of filament or microtubule movement, a method for starting and stopping, and a way to load and unload their cargo.

Several methods for confining the motile components of the system (actin filaments or microtubules) and directing their motion have been used in past studies. Two of the most commonly used methods are chemical[13,14] and topographical patterning of surfaces[15-20]. Chemical patterning typically results in varying surface hydrophobicity, where some regions of the surface favor adsorption of the motor protein over other regions. Topographical patterning can be achieved using direct lithography techniques[15,16,18,19] or replica molding[17,20]. In some cases, chemical and topographical patterning methods are used together. A few groups have also used enclosed channels for confinement of microtubules[21-23]. To more specifically guide filament

or microtubule motion, some techniques such as PMMA gratings[24] and electric fields[22,24] have been developed. Unidirectional motion of microtubules has been achieved with directional rectifiers resembling arrowheads or heart-shapes[16,25].

There are also a few different approaches to starting and stopping filament or microtubule movement. Stoppage can occur due to a lack of ATP or by the inhibition of the hydrolysis of ATP. Introduction of caged ATP into the motility assay has resulted in cycles of starting and stopping microtubules by using UV light exposure to release a portion of the ATP[17]. The microtubules begin to move at a high velocity and gradually slow to a stop when the ATP is used up, at which point another exposure to UV light is necessary to start the movement again. Blebbistatin has also been used to manipulate myosin ATPase activity in motility assays[26,27]. Blebbistatin is a small-molecule, high-affinity, noncompetitive inhibitor specific for most forms of myosin II[28] and can be photoinactivated by illumination with "blue" light[26], allowing for reversible starting and stopping. A different method of control uses a dendrimer with peripheral guanidinium ions that has been found to inhibit motility of actin by preventing dissociation of the actomyosin complex[29]. This effect was also found to be reversible, with motility resuming after washing the flow cell with ATP buffer. In another study[30], removal of antioxidants (the glucose oxidase-catalase system) and reducing agents [dithiothreitol (DTT)] from the motility buffer caused motility to cease, with motility resuming after the components were re-introduced. This behavior was thought to be due to a reversible oxidative modification of the myosin structure, most likely a disulfide bond.

Biomolecular motor systems have been successful at carrying several different types of cargo, and some methods for loading and unloading cargo have been developed. Streptavidin-coated quantum dots have been transported by actin filaments[31]. Actin bundles have been used to

5

carry streptavidin- and biotin-coated beads[27], liposomes[32], and *E. coli* cells[32]. Microtubules labeled with single-stranded DNA have been able to load and unload polystyrene beads[33], quantum dots[33], gold nanoparticles[34], and liposomes[35] labeled with complementary single-stranded DNA.

Combining all of these features into one integrated microfluidic device, containing channels with measurements of width and height that are on the order of microns, could provide the best means to both confine the biomolecular motor system and incorporate a method for starting and stopping, as well as loading and unloading cargo. Incorporating biomolecular motors into microfluidic devices for use with cargo transport could enable the production of new analytical devices that operate on a very small scale[36]. The small dimensions of these devices can yield several benefits, including: lower production and usage costs, smaller quantities of reagents and analytes, shorter analysis time, and less waste[37]. Using biomolecular motors for nanotechnology applications within a microfluidic device has several advantages. Typically when chemical patterning techniques are used to contain the motor system, the motor protein favors adsorption to only one portion of the pattern, restricting motility to that area. However, because physical barriers are not present, the filaments or microtubules are free to fall off the edge of the track or diffuse away. When topographical patterning is used, motility is often in a recessed track with walls that act as physical barriers and aid in the containment, but some filaments or microtubules may still climb the walls and be lost. In a microfluidic device, the walls and ceiling of the small channels act as barriers to completely contain the filaments or microtubules. It is also possible to create a wide variety of microfluidic channel designs that suit specific needs. Additionally, because there are methods to seal the device, it could be possible for the device to be stored without loss of function of the proteins.

Motility of microtubules over a kinesin-coated surface has been achieved in enclosed microfluidic channels[21-23], but to our knowledge, no one has successfully introduced the actin-myosin system into an enclosed channel. In this work, we have sought to incorporate the actin-myosin biomolecular motor system into a device containing PDMS/glass microfluidic channels. The parameters that must be changed and/or optimized when transitioning from the glass flow cell used in standard motility assays to a microfluidic device, as seen in Figure 5, have been addressed.
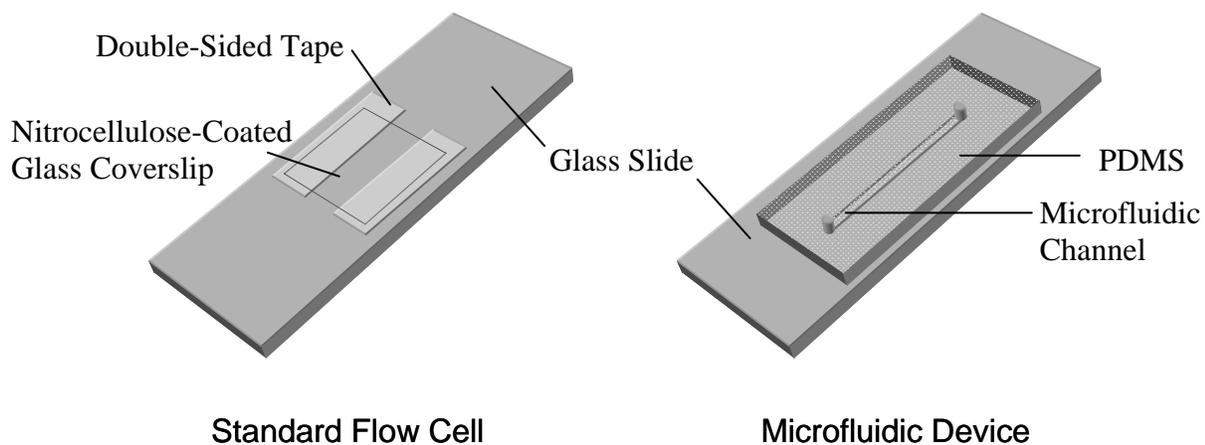
Figure 5. Comparison of a standard flow cell and a rudimentary microfluidic device.

<u>**Experimental Methods**</u>

<u>Materials</u>

HMM, actin acetone powder, fascin, glucose, glucose oxidase, catalase, and ATP were obtained from Dr. Eric Blough's lab. Sodium bicarbonate (Sigma-Aldrich) and potassium chloride (Sigma Chemical Company) were purchased. An Eppendorf Refrigerated Centrifuge 5403 and a Beckman Optima LE-80K Ultracentrifuge were used in making F-actin. Rhodamine phalloidin from Invitrogen (Molecular Probes R415) and Cytoskeleton (PHDR1) was used to

label F-actin. A Thermo Spectronic Genesys 10 Vis spectrophotometer was used to perform Bradford assays. Imidazole (99+%, crystalline) from Acros Organics was a motility buffer component. FisherFinest Premium Cover Glasses (18mm x 18 mm, No. 1) or Fisherbrand Microscope Cover Glass (18mm x 18mm, No.2) from Fisher Scientific, Pearl frosted microscope slides from T&Q Industries, and NICETACK 15mm x 20m double-sided tape (NW-15) from Nichiban were used to construct flow cells. 2% collodion (in isoamyl acetate) and isoamyl acetate (98%) from Sigma-Aldrich were used to create nitrocellulose-coated cover glass. Coomassie (Bradford) Protein Assay Reagent and Albumin (BSA) Standard Ampoules (2 mg/mL) were purchased from Thermo Scientific. Methylcellulose was purchased from Fisher Science Education.

A Sylgard 184 Silicone Elastomer Kit from Dow Corning Corporation containing Sylgard 184 Silicon Elastomer Base and Sylgard 184 Silicon Elastomer Curing Agent was used to make PDMS. Silica wafers with SU-8 photoresist patterns were ordered from the Stanford Microfluidics Foundry as master molds. A punch (CR0350255N20R4) was purchased from Technical Innovations for punching input holes in PDMS. Dichloromethane (Macron Chemicals), pentane (Fisher Scientific), and toluene (EMD Chemicals) were all used for removing contaminants from PDMS. Fisherbrand Microscope Cover Glass (24mm x 40mm, No. 2) was used as the floor of the device. Ethyl alcohol (200 Proof) from PHARMCO-AAPER and isopropanol (Acros Organics) were used for cleaning PDMS and glass. Concentrated sulfuric acid (Fisher Scientific) and hydrogen peroxide (35 wt.% in water) from Acros Organics were used to make piranha solution for cleaning glass. A plasma cleaner (SN: PDC32G1051452) was purchased from Harrick Plasma. TMCS from Thermo Scientific and 3-aminopropyltrimethoxysilane (Aldrich) were used for functionalizing glass surfaces. A Pacific

Nanotechnology Nano-R AFM was used to study the glass surfaces. EZ-Link® Sulfo-NHS-LC-Biotin was purchased from Thermo Scientific.

A Cheminert six-port injector from VICI, a KD Scientific single syringe infusion pump (KDS100), and a KD Scientific two syringe infusion pump (KDS200) were used to introduce solutions into the device. A 25 µL Hamilton syringe was purchased to inject solutions. Stainless steel tubes (0.025" OD x 0.017" ID x 0.500" long) were purchased from New England Small Tube Corporation. A Nikon Diaphot 300 microscope, an Olympus UVFL100 objective, and a Hamamatsu Orca-R^2 digital CCD camera were used for imaging.

Standard Actin Motility Assay

Prior to proceeding with experiments to obtain actin motility in a microfluidic channel, a positive control for actin motility had to be established. Imidazole buffer (25 mM imidazole, 25 mM KCl, 2 mM MgCl$_2$, 0.2 mM CaCl$_2$, pH: 7.0) was made for use as the motility buffer. F-actin was obtained by polymerization of G-actin using a standard protocol (see Appendix A-I). F-actin was also labeled with rhodamine phalloidin for stabilization and visualization (Appendix A-II). If desired, actin was bundled using the protein fascin (Appendix A-III). HMM was obtained, and a Bradford assay was performed to determine concentration (Appendix A-IV). A flow cell was constructed out of a glass slide and a nitrocellulose-coated coverslip, and standard motility assay procedures were followed (Appendix A-V). Standard motility assays were performed at regular intervals to ensure that HMM was active and that good actin motility could be visualized.

Designing Microfluidic Masters

AutoCAD 2007 and AutoCAD 2012 were used to create microfluidic channel designs (Figure 6). Figure 6–A is a simple design of two perpendicular channels forming an intersection. Figure 6–B is a modified "Y"-shaped design meant for establishing laminar flow with three

inputs and one output. A gradient of several straight channels with widths ranging from 400 µm to 1000 µm (Figure 6–D) was designed to investigate the influence of the flow velocity inside the microfluidic channel on obtaining actin motility. Figures 6–C, 6–E, and 6–F are all combinations of Figures 6–A and 6–B. As the most complex design, it was created for experiments investigating starting and stopping actin motility inside a microfluidic device.
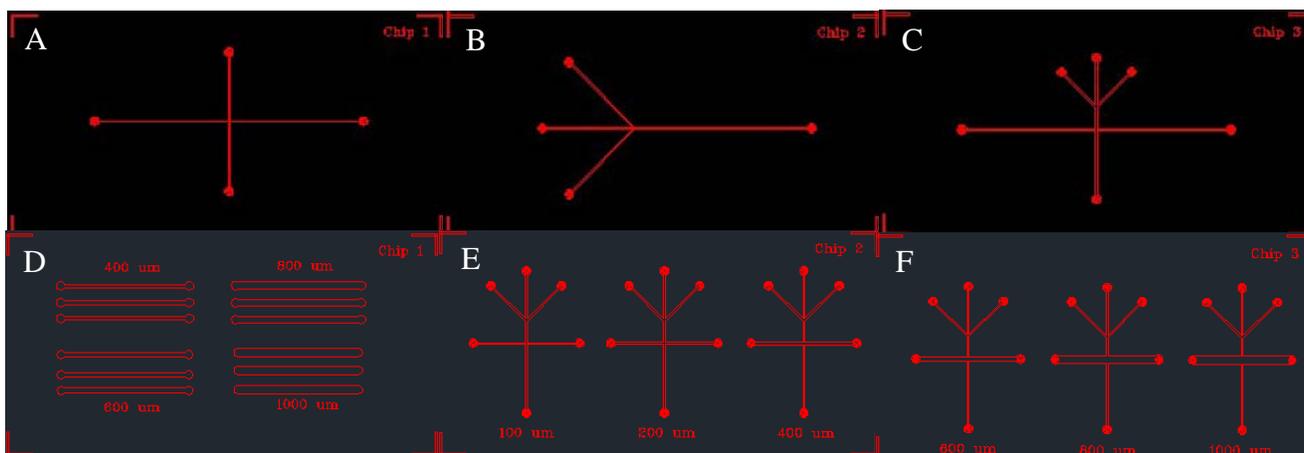
Figure 6. AutoCAD 2007 (top) and AutoCAD 2012 (bottom) designs for photoresist masters used to create microfluidic channels in PDMS.

The designs were sent to the Stanford Microfluidics Foundry to create masters (silicon wafers with SU-8 photoresist patterns). A photomask was created by printing the desired design on transparency film using a high resolution printer (20,000 dpi). SU-8 photoresist was spin-coated onto a silicon wafer, and the photomask was placed over the wafer. The photoresist was then exposed to UV light, but only in the areas where the photomask was transparent. In the case of SU-8, a negative photoresist, the UV light exposure caused cross-linking. In the regions where SU-8 was not exposed to UV wavelengths, the SU-8 was removed with a developer solution. This procedure resulted in raised channel features, which can be used to mold PDMS.
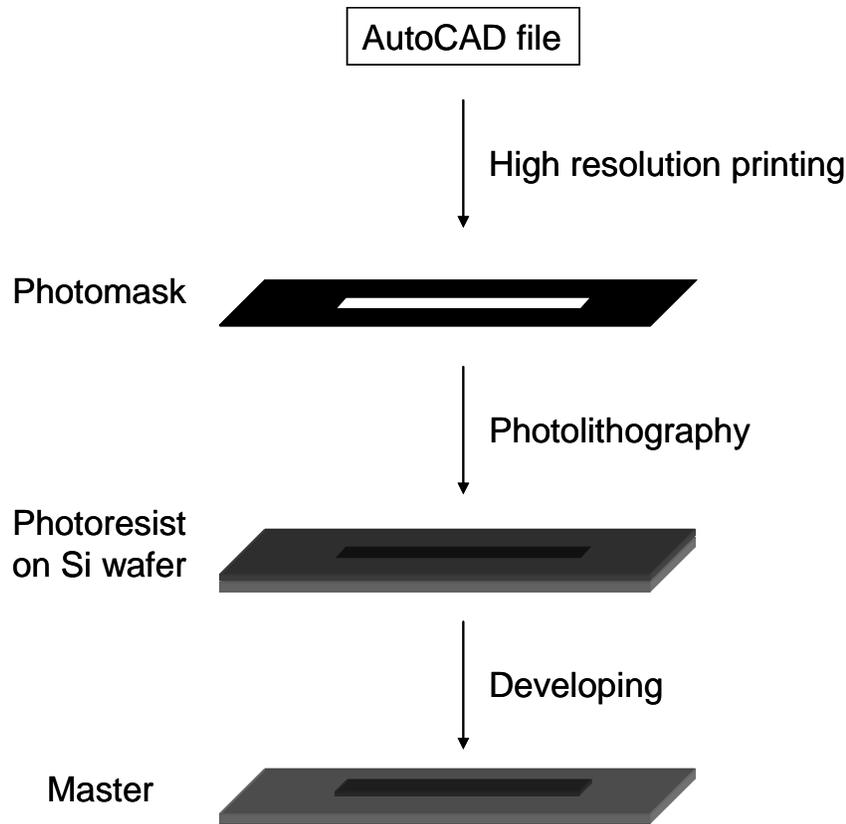
Figure 7. Steps for creating a photoresist master using photolithography.

Making PDMS Molds

To make the PDMS portion of the device, Sylgard 184 Silicone Elastomer Base and Sylgard 184 Silicone Elastomer Curing Agent were mixed in a 10:1 ratio by mass. A vacuum desiccator was used to remove gas from the mixture. The pre-polymer mixture was poured over a master in a Petri dish and placed in a 75°C oven for about two hours. The mold was removed from the Petri dish and separated from the master. Using a punch housed by a drill press, holes were punched in the PDMS to create inputs for external tubing. To remove remaining pre-polymer components, the mold was sonicated in a solvent that swelled the PDMS (i.e. toluene, methylene chloride, pentane), followed by a solvent that allowed the PDMS to return to its original shape (i.e. ethanol or isopropanol). In early experiments, molds were sonicated in

toluene two times for at least five minutes, then in ethanol or isopropanol two times for at least five minutes. In later experiments, 5 minute sonications in methylene chloride, pentane, and isopropanol were performed, in that order, and the cycle was completed three times. This technique was based on the procedure of Runge *et al.*[38], in which methylene chloride and pentane were used to remove remaining platinum catalyst. After the washing steps, the PDMS mold was placed in a 75°C oven overnight to remove any remaining solvent.

Cleaning Glass Surfaces

In order to clean the glass surface of the device, it was rinsed with water, sonicated in ethanol or isopropanol for at least five minutes, and dried with nitrogen gas. The glass was placed in a plasma cleaner for one minute at about 200 mtorr for additional cleaning. Alternatively, the glass was sonicated in deionized water for at least five minutes, and then cleaned in piranha solution (concentrated sulfuric acid and 30% H_2O_2 in a 7:3 ratio) for one hour. *Caution: piranha solution is a highly corrosive acidic solution that can react violently with organic materials. Do not store in a closed container, and use appropriate safety precautions.* When removed from the piranha solution, the glass was rinsed with deionized water and dried with nitrogen gas.

Atomic Force Microscopy of Cleaned Surfaces and Image Analysis

Glass coverslips were cleaned using variations of the two methods described above. One coverslip was rinsed with water, sonicated in ethanol, rinsed with isopropanol, and dried with nitrogen gas. Another was soaked in piranha solution (7:3 ratio of concentrated sulfuric acid : 30% hydrogen peroxide) for one hour, rinsed with deionized water, and dried with nitrogen gas.

Surfaces were imaged using a Pacific Nanotechnology Nano-R AFM. A tapping mode probe made of single crystal silicon with a radius of less than 10 nm was used. The working

frequency range for the tip was 200-400 kHz. To obtain an AFM image, the laser was aligned with the tip and the detector. A frequency sweep was performed to identify the resonance frequency for the tip. The tip was brought into feedback with the sample, and the setpoint and gain settings were modified to produce an acceptable line scan. A 20x20 μm^2 scan was taken of each surface. The scan rate was 1 Hz and the resolution was set to 512 pixels x 512 pixels for all scans collected.

Images were analyzed using Pacific Nanotechnology Nanorule+ software. Multiple leveling steps were performed on each image due to tilt and bowing that were introduced by the scanner. 1st order, 2nd order, and 3rd order 1D horizontal leveling were performed, followed by 1st order, 2nd order, and 3rd order vertical leveling. If large particles were visible in the image, these were excluded prior to each leveling. Surface roughness measurements were then taken for the images. Particle counts were performed using ImageJ software. The threshold for each image was set at the pixel intensity corresponding to 3 nanometers above the intensity value at the maximum of the image's histogram. Each image was converted to a binary image and the "Analyze Particles" function was used to obtain the particle count.

Functionalizing the Glass Surface of a Microfluidic Device

Glass surfaces were functionalized with either 3-aminopropyltrimethoxysilane or TMCS. To functionalize a clean glass coverslip with 3-aminopropyl-trimethoxysilane, the glass was placed inside a glass jar along with an aluminum foil "bowl" containing two to three drops of the amine-terminated silane. The lid was sealed, and the jar was placed in a 100°C oven for one hour. The surface was rinsed with ethanol and water following deposition. The same method was used to functionalize the glass surface with TMCS. To test the covalent bonding between glass functionalized with each silane and PDMS, a PDMS surface was activated by a plasma cleaner,

placed in contact with the functionalized glass, and heated in a 75°C oven for at least 15 minutes. After removal from the oven, tweezers were used to attempt to remove the PDMS from the glass surface in order to test the strength of the bond formed, if any. Actin-myosin motility assays were also performed using both treated surfaces.

In order to perform functionalization of microfluidic channels after a device had been constructed, the vapor deposition method outlined above was modified. TMCS vapor was drawn from the headspace of a vial containing a few drops of liquid TMCS, and then introduced into the microfluidic channel, which was plugged to contain the TMCS vapor. Actin-myosin motility was performed on coverslips functionalized by vapor depositing TMCS in a similar way to determine the amount of time needed for deposition. Solution deposition of TMCS was also investigated by attempting functionalization of glass coverslips with TMCS in either water or ethanol. Different concentrations of TMCS in ethanol (1%, 2% and 5%) were used to treat glass surfaces, which were tested with the standard actin motility assay. In all further experiments with functionalized glass, the microfluidic channels were incubated with a solution of 5% TMCS in ethanol for 15 minutes immediately after the device was constructed.

Constructing Microfluidic Devices

To bond the PDMS and glass together in our initial hybrid microfluidic device, a plasma cleaner was used to oxidize the surface of the PDMS with the channel molds. If glass was cleaned with piranha solution immediately prior to this step, no plasma treatment of the glass was necessary. Otherwise, the glass was also placed in the plasma cleaner. The surfaces were placed face up in the plasma chamber and treated with a plasma created with room air at about 200 mtorr for 20 to 40 seconds. The surfaces were then removed and placed in contact with one

another immediately. Pressure was applied to ensure that the entire surface was in contact. The device was placed in a 75°C oven for at least 15 minutes to help strengthen the bond.

1)
CH₃ CH₃ CH₃ CH₃ CH₃ CH₃ CH₃
Si Si Si Si Si Si Si
PDMS

Plasma oxidation →

OH OH OH OH OH OH OH
Si Si Si Si Si Si Si
PDMS

2)
Glass Slide
Si Si Si Si Si Si Si
OH OH OH OH OH OH OH

↓

OH OH OH OH OH OH OH
Si Si Si Si Si Si Si
PDMS

→

Glass Slide
Si Si Si Si Si Si Si
O O O O O O O
Si Si Si Si Si Si Si
PDMS
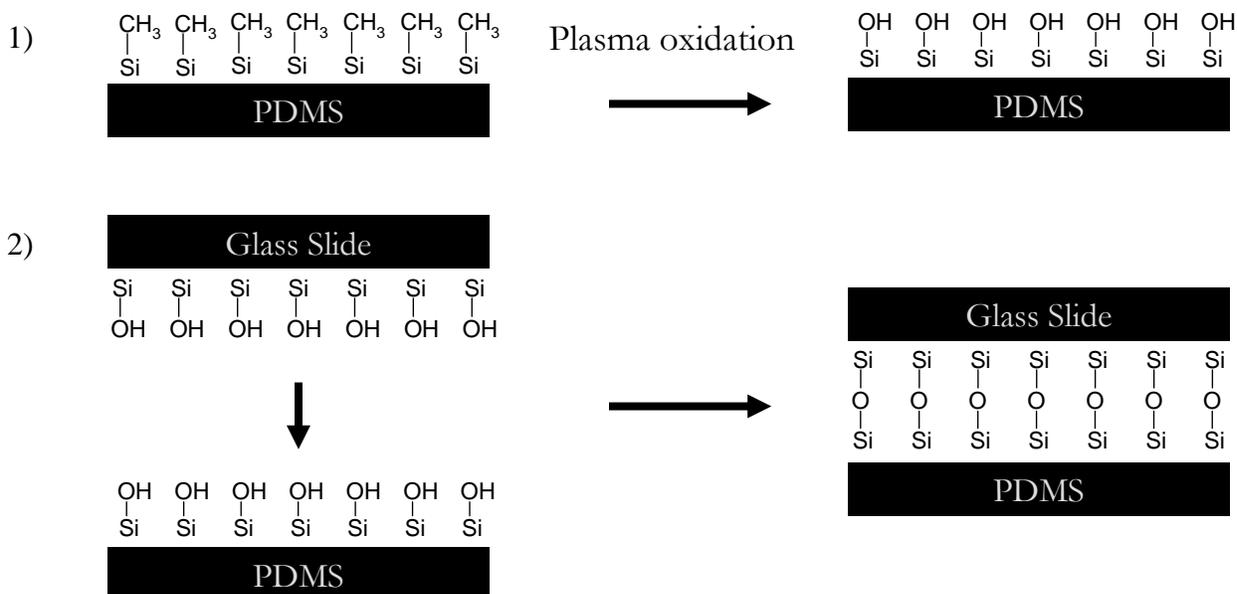
Figure 8. Chemical reactions involved in bonding PDMS to glass.

After a lack of motility in the initial microfluidic devices, a new method for constructing the devices was developed. After the washing procedures described earlier, the PDMS mold was placed channel-side up in a plasma cleaner and treated for 20 minutes. Additional PDMS pre-polymer was mixed and spin-coated on a silica wafer (approximately 80 µL, ramped at 500 rpm/sec to a speed of 7000 rpm/sec for 5 minutes). The PDMS mold was stamped against the silica wafer so that the surface was evenly coated with pre-polymer. The PDMS mold was carefully lifted up and placed on a piranha-cleaned glass coverslip. The device was placed in a 75°C oven for about 1 hour.

15
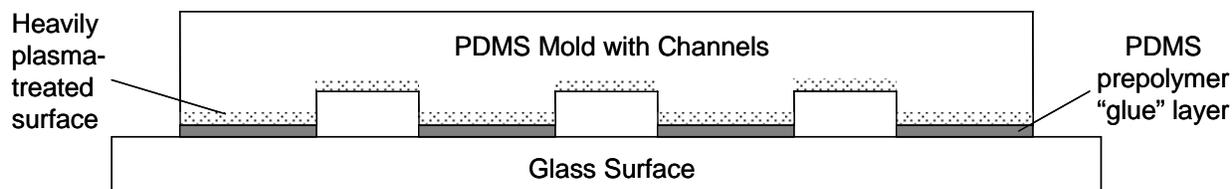
Figure 9. Microfluidic device constructed using a PDMS "glue" layer.

Actin Motility Assay in a PDMS/Glass Flow Cell

The standard motility assay flow cell described above was modified so that a PDMS slab replaced the glass slide used to construct the cell. Experiments were performed with hydrophilic PDMS (treated with an air plasma for 40 seconds), functionalized PDMS (treated with an air plasma and exposed to TMCS), and PDMS with reduced oxygen permeability (treated with an air plasma for 20 minutes). Both nitrocellulose-coated coverslips and TMCS-treated coverslips were used as motility surfaces with this type of flow cell. The standard motility assay protocol was followed (Appendix A-V). Methylcellulose (0.3% - 0.6%) was included in the ATP solution for these experiments.

Actin Motility Assay in a Modified Microfluidic Device

A PDMS mold with channels was trimmed in such a way that one end was cut off of each channel, leaving one open end and one end with a punched hole for a tubing connection. Both the standard method (plasma treatment) and the method using a pre-polymer "glue" layer were used for constructing these devices. To perform the motility assay, solutions were pipetted at the edge of the device next to the open end of the channel, and a syringe was attached via tubing to the other end of the channel. Pulling the syringe plunger back resulted in a vacuum, which pulled the solutions through the channel. Solution volumes and incubation times from the standard motility assay procedure were used. Both 0.3% methylcellulose and 10 mM DTT were present in

16

the ATP solution. The channel was imaged using fluorescence microscopy after the addition of the ATP solution.
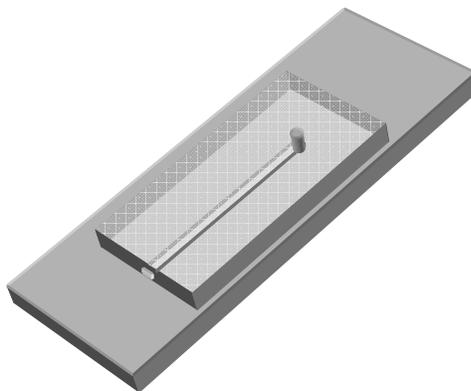
Modified Microfluidic Device

Figure 10. Schematic of a modified microfluidic device with an open-ended channel.

Reactions at the Surface of a Microfluidic Device (with Laminar Flow)

A glass coverslip was cleaned using a plasma cleaner and functionalized with 3-aminopropyltrimethoxysilane as described above. A PDMS mold with a cross-shaped channel pattern was exposed to an air plasma for 20 seconds and bonded to the functionalized glass to complete the device. As depicted in Figure 11-A, phosphate buffer was introduced into channels 2 and 3 at a flow rate of 1.0 mL/hr. Then, 0.01 mg/µL NHS-LC-biotin (an *N*-hydroxysulfosuccinimide ester of biotin, which contains an amine-reactive group) in phosphate buffer was started flowing in channel 1 at a flow rate of 0.1 mL/hr. The phosphate buffer flow in channels 2 and 3 was decreased to 0.2 mL/hr, and the solutions were allowed to flow for 30 minutes. This setup created a sheath flow beginning at the intersection and exiting out channel 4. The biotin flow was stopped, and the device was washed with buffer for 15 minutes at a rate of 2.0 mL/hr. The remaining surfaces were coated with BSA by introducing a 1.0 mg/mL BSA solution into channel 1 and allowing it to flow out of all three other channels for 30 minutes at a

17

rate of 0.1 mL/hr. The BSA blocked non-specific binding of neutravidin-FITC (fluorescein iso-

thiocyanate) to the surface. Channels 1 and 4 were then used as buffer inputs, and the washing

step was repeated. Next, the buffer flow rate was lowered to 1.0 mL/hr, and 10 µg/mL

neutravidin-FITC was flowed through channel 3 at a rate of 0.1 mL/hr (Figure 11–B). The buffer

flow rate was decreased to 0.2 mL/hr, and the solutions were allowed to flow through for 30

minutes, with all solutions exiting channel 2. The device was then rinsed again with buffer and

imaged using fluorescence microscopy.
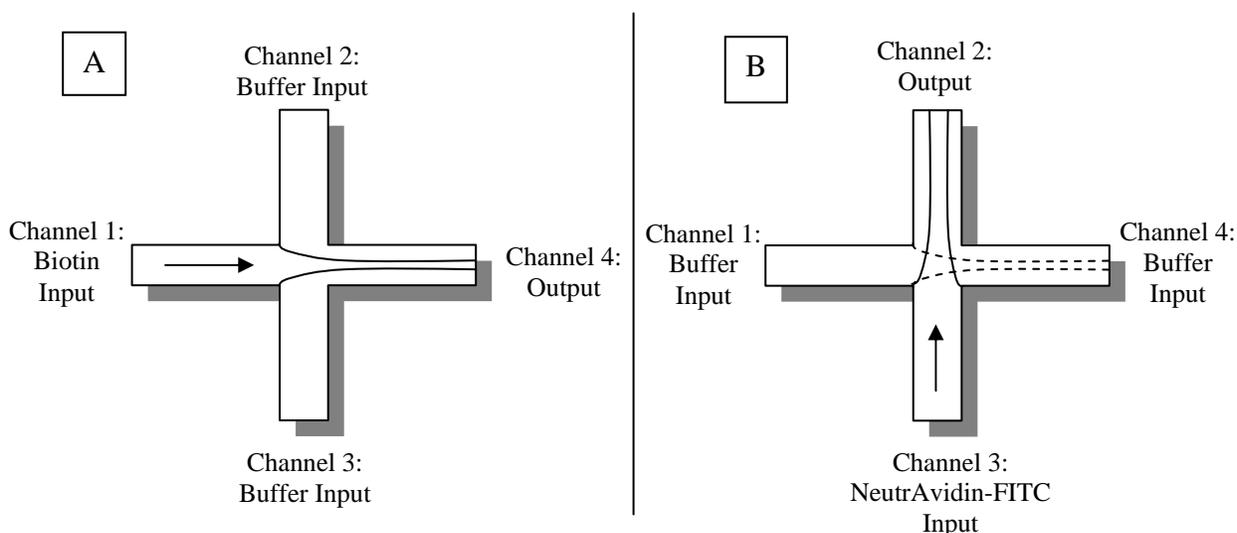
Figure 11. Experimental design for testing reactions at the surface of a microfluidic device.

Introducing Actin-Myosin System into Microfluidic Device

      To introduce all of the necessary components for the actin-myosin system into the

microfluidic device, we utilized a six-port injector. In this setup, buffer was flowing from a

syringe pump into the device continuously. An injection port connected to a sample loop allowed

the necessary reagents to be injected into the device. HMM was added to the device first,

followed by BSA, which blocked any surfaces that were not coated by HMM. The actin was then

injected and bound to the myosin heads present on the surface. Fluorescent microscopy was used to visualize actin filaments bound to the device surface.

To optimize the conditions for blocking the channels with BSA, fluorescently-labeled BSA was introduced into microfluidic channels using various flow rates and exposure times and imaged using fluorescence microscopy. The fluorescence signal was interpreted to estimate an exposure which saturated the channel floor with BSA. Unlabeled BSA was then introduced to a channel using the optimized conditions (30 minutes of exposure to a 1 mg/mL BSA solution at a flow rate of 0.02 mL/hr). Actin was then flowed through the channel, and the channel floor was imaged using fluorescence microscopy. In another channel, HMM was deposited, followed by BSA blocking using the same conditions. Actin was introduced and the channel was imaged.

Laminar Flow

To demonstrate laminar flow, a microfluidic device was set up with three inputs and one output channel. Red, blue, and green dye solutions were flowed into three inputs on the device. The flow rates were initially set at 0.05 mL/hr. An optical microscope was used for observation.

In another experiment, a microfluidic device with the channel pattern shown in Figure 6–C was constructed. Blue dye was introduced into the middle of the "Y"-shaped portion with buffer flowing through the inputs on either side of the dye to create a sheath flow. The result was again observed with an optical microscope.

Results and Discussion

Atomic Force Microscopy of Cleaned Surfaces and Image Analysis

In our early actin-myosin motility experiments using TMCS-derivatized glass, the glass was cleaned with water, ethanol, and isopropanol. Based on several AFM scans, it appeared that these surfaces were still quite contaminated. Particles on the surface could interfere with the

chemistry of functionalizing the surface, leading to less than optimal results if HMM cannot adsorb to the surface in a way that supports motility. Due to this result, a new cleaning method was tested, in which glass coverslips were cleaned with piranha solution. Figure 12 shows a comparison of two glass surfaces cleaned via the different methods. Comparisons of both the scan images and the RMS surface roughness measurements show that far less contamination was evident on the glass cleaned with piranha solution. To ensure that the glass was as free of contamination as possible, piranha solution was adopted as the primary cleaning method for the remainder of the TMCS-coated glass experiments.

RMS Surface Roughness: 1.13 nm
Particle Count: 64

RMS Surface Roughness: 0.30 nm
Particle Count: 4
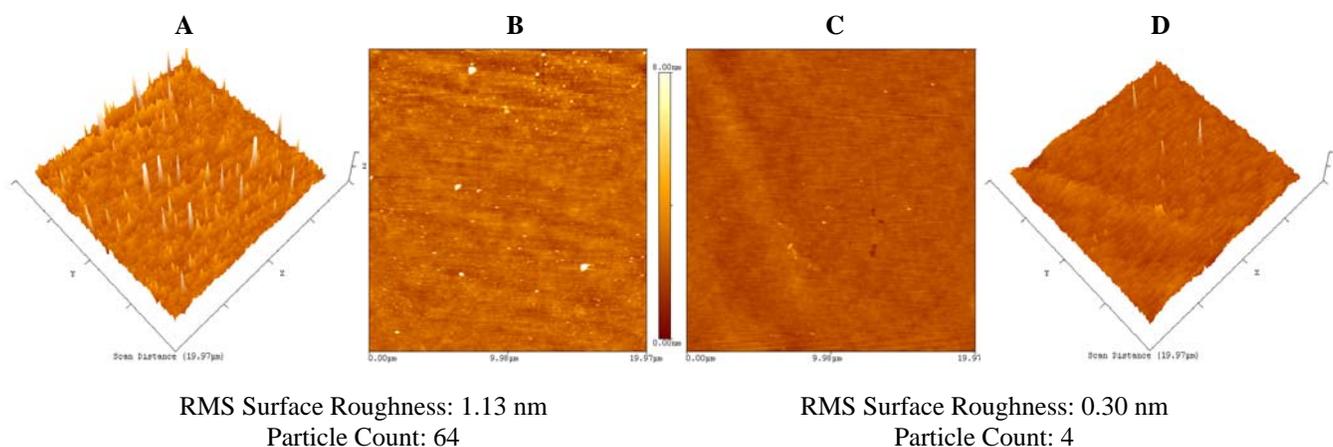
Figure 12. AFM images of glass coverslips cleaned with two different methods. 3D (A) and flat (B) representations of a 20x20 μm^2 scan of glass cleaned by washing in water, ethanol, and isopropanol. Flat (C) and 3D (D) representations of a 20x20 μm^2 scan of glass cleaned using piranha solution. The images were set to a common z-height range for comparison. The original ranges were 83.23 nm for the left image and 9.71 nm for the right image.

Functionalizing the Glass Surface of a Microfluidic Device

One constraint on our system was the requirement of a surface which would both bind myosin and support the motility of actin filaments or bundles. The standard nitrocellulose surface could not be used with a microfluidic device because PDMS cannot form an irreversible seal

with the glass surface if it is coated with nitrocellulose. Due to the viscosity of the nitrocellulose solution, it would be very difficult to flow nitrocellulose through a microfluidic channel and leave only a thin coating on the channel walls after it was constructed. Therefore, another functionalization method was required to create a surface that supports motility within the device.

We functionalized glass surfaces with either 3-aminopropyltrimethoxysilane or TMCS and tested the ability of the modified glass surfaces to both support actin motility and covalently bond with plasma-treated PDMS. It was determined that the TMCS-functionalized glass surfaces did not form permanent bonds to the PDMS, but the surfaces treated with 3-aminopropyltrimethoxysilane did. While it would have been convenient to have the ability to functionalize the glass prior to device assembly, actin-myosin motility observed during standard motility assays was limited on the 3-aminopropyltrimethoxysilane-treated surfaces. Better motility was observed on the TMCS-treated surface so TMCS was chosen as the reagent for functionalization.

A disadvantage of using TMCS was the requirement that the device be assembled before the glass surface was treated. For this reason, a method for vapor depositing TMCS inside the microfluidic channels was developed. A series of myosin-actin motility experiments showed that incubating a glass coverslip with TMCS vapor for one hour yielded some motility, but increasing the incubation time to four hours yielded motility over a greater area of the treated surface. While these large scale test experiments yielded positive results, it was difficult to test the quality of the surface inside of a microfluidic channel once the TMCS was deposited. Therefore, we could not confirm that a TMS-functionalized surface was being achieved in our device. Vapor

deposition was also a very time consuming process. For these reasons, we chose to switch to solution deposition of the TMCS.

By using a solution deposition method to functionalize the glass surface of our microfluidic device, it was possible to confirm that TMCS solution was coming in contact with the interior of our channels. This method of deposition required finding a solvent for TMCS that would be compatible with PDMS. PDMS swells when it comes in contact with many solvents, such as pentane, methylene chloride, and toluene. These solvents had to be avoided to prevent distortion of our channels. Also, retention of some solvents in the PDMS could be harmful to the myosin and actin proteins. When water was used as a solvent, the treated glass appeared to maintain its hydrophilicity (based on observation of water surface contact angle), indicating that TMCS had not reacted significantly with the hydroxyl groups on the glass. This lack of surface functionalization was most likely due to the rapid hydrolysis of TMCS by water, resulting in trimethylsilanol. Ethanol proved to be an acceptable solvent, however, with the treated glass surface becoming much more hydrophobic. While ethanol could still react with TMCS, it still allows functionalization of the glass, especially when higher concentrations of TMCS are used. Testing of various concentrations of TMCS in ethanol (1%, 2% and 5%) found that motility was most consistent on glass treated with 5% TMCS solution for 15 minutes, so this method was chosen as the standard procedure for the remaining experiments.

Actin Motility Assay in a PDMS/Glass Flow Cell

One major impediment to achieving and controlling actin translation within a microfluidic device is the change in materials needed for a flow cell as opposed to a microfluidic device. Since a flow cell is open-ended, it can be easily constructed from two glass surfaces held together by something such as double-sided tape. A microfluidic device, however, needs to be

sealed so that the fluid being pumped through the channels remains contained. While microfluidic devices can be fashioned from glass, it is a difficult and time consuming process. Often, the channels are molded using a polymer, because it is much easier than etching techniques. PDMS is one polymer that is frequently used. There are many advantages to using PDMS for microfluidic applications. It provides good reproducibility of micron-sized features and can create seals through the formation of covalent bonds (after treatment with air plasma). It is also nontoxic and optically transparent[37]. However, PDMS is problematic in one respect. It is much more permeable to oxygen than is glass. The oxygen permeability of neat PDMS has been reported as 800 Barrers (1 Barrer = 10^{-10} cm^3 (STP) $\cdot$ cm (cm$^2 \cdot$ s $\cdot$ cm Hg)$^{-1}$)[39].

Initially, we attempted to use both hydrophilic PDMS surfaces (plasma treated for 40 seconds) and functionalized PDMS surfaces (plasma treated for 40 seconds and exposed to a 5% TMCS solution for 15 minutes) to construct flow cells. Our experiments showed that actin motility was achieved in the PDMS/glass flow cells when either 0.3% or 0.6% methylcellulose was present in the ATP solution, but only for a short time after illumination (Figure 13). Upon illumination, motility quickly ceased. Motility was present on both nitrocellulose-coated and TMCS-treated glass. Although motility was limited, these results proved that the proteins remained functional after introduction into a cell constructed partially of PDMS. The results were similar to other studies where oxygen was cited as an inhibitor of motility[30,40,41].
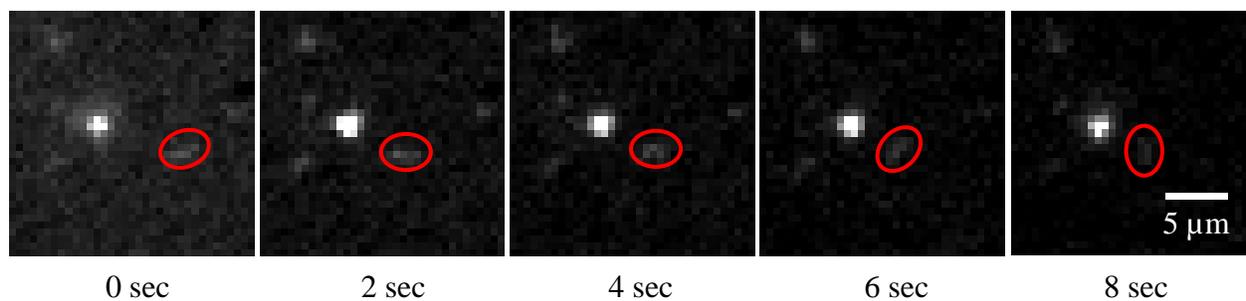
23

| 0 sec | 2 sec | 4 sec | 6 sec | 8 sec |

Figure 13. Motility of a rhodamine-labeled actin filament in a PDMS/glass flow cell that had not been treated to reduce oxygen permeability. A nitrocellulose surface was used and 0.3% methylcellulose was present in the ATP solution.

Nalabotu et al.[30] showed that oxidative conditions (removal of both the glucose oxidase-catalase antioxidant system and the reducing agent DTT) in a standard motility assay flow cell caused actin filament motility to cease immediately. This effect was attributed to an oxidative modification to the myosin. PDMS has also been shown to inhibit motility of the kinesin-microtubule biomolecular motor system[40,41], and it is thought to be due to the presence of oxygen. Brunner et al.[40] achieved motility of microtubules on a kinesin-coated surface in a flow cell constructed of PDMS and glass when illumination was limited, but upon continuous intense illumination (such as that needed for fluorescence microscopy), microtubules were found to be very unstable, with disintegration occurring within about 30 seconds. This observation coincided with photobleaching of the microtubules. The results were very similar to those encountered when a glass flow cell was used without the oxygen scavenging system of catalase and glucose oxidase. This similarity suggested that the presence of oxygen in the PDMS system was the problem. Kabir et al.[41] also found that kinesin-microtubule motility ceased rapidly upon illumination when PDMS was present, due to its high oxygen permeability. After development of a sealed chamber that placed the flow cell in a nitrogen atmosphere, good motility was observed with PDMS. These studies clearly indicate that the permeability of PDMS to oxygen is a significant hindrance to achieving motility with a biomolecular motor system.

24

To combat this problem, we established a procedure for eliminating the introduction of oxygen into the flow cell. Houston *et al.*[42] showed that the permeability of PDMS to oxygen can be reduced by plasma treatment. Reductions in the oxygen permeability coefficient of PDMS ranged from 40-80% when argon or oxygen plasmas were used. This decline is due to the formation of an oxidized surface layer of SiO_x that can be up to 130-160 nm thick[43]. Due to this effect, we chose to treat the surface of the PDMS slab used to make the flow cell with an air plasma for an extended period of time (20 minutes). When a motility assay was performed, long-lasting motility was visualized (Figure 14). Based on the observed fraction of moving bundles, the average velocity of movement, and the length of time that the bundles were motile, the motility achieved was comparable to standard motility assays with a glass flow cell. This result confirmed that the actin motility was being inhibited by the presence of oxygen and that extended plasma treatment was able to significantly reduce the permeability of the PDMS to oxygen.
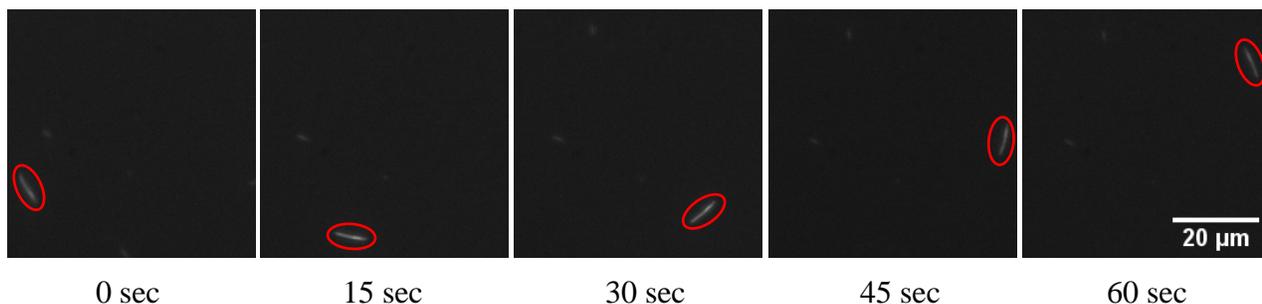

| 0 sec | 15 sec | 30 sec | 45 sec | 60 sec |

Figure 14. Actin bundle motility in a PDMS/glass flow cell with reduced oxygen permeability. The PDMS surface of the flow cell was treated with an air plasma for 20 minutes. Motility was visualized until significant photobleaching had occurred (an additional 60 seconds from the last image of this sequence).

<u>Actin Motility Assay in a Modified Microfluidic Device</u>

After good quality motility was obtained in the PDMS/glass flow cell, we sought to develop a way to use the same principles to obtain motility in a microfluidic channel. Because heavily plasma-treated PDMS does not bond well to glass, we needed a way to form a good seal between the heavily treated PDMS and glass. To do this, we chose to spin-coat a thin layer of PDMS pre-polymer onto a silica wafer, place our heavily plasma-treated PDMS mold (containing our channel pattern) down onto the wafer, and lift it away again, leaving a thin film of pre-polymer on the surface. The mold was then placed onto a clean glass coverslip and heated to allow the pre-polymer to polymerize. During polymerization of the pre-polymer, bonds should form to hydroxyl groups on both the PDMS mold and the glass, yielding a sealed device.

We used this method of constructing a device to make a modified microfluidic device which had channels with one hole punched for tubing access and one open end. In this way, we were able to reproduce the standard motility assay flow cell procedure. Solutions were pipetted onto the glass surface of the device at the open end of the channel. A syringe was connected via tubing to the punched hole and was used to pull the solutions through the channel. The same volumes, concentrations, and incubation times were used as in the standard assay. When this experiment was performed using 800 µm wide channels, actin motility was obtained (Figures 15, 16).

Although plasma treatment did significantly improve the motility in the modified microfluidic device, it was not as dramatic an improvement as that of the PDMS/glass flow cell. The fraction of motile actin and the duration of motility were still not of the quality of a standard flow cell. This outcome suggests that the plasma treatment was not as effective at reducing the

oxygen content in the PDMS microfluidic channels as it was for the PDMS surface in the flow cell. Reasons for this difference need to be further investigated.
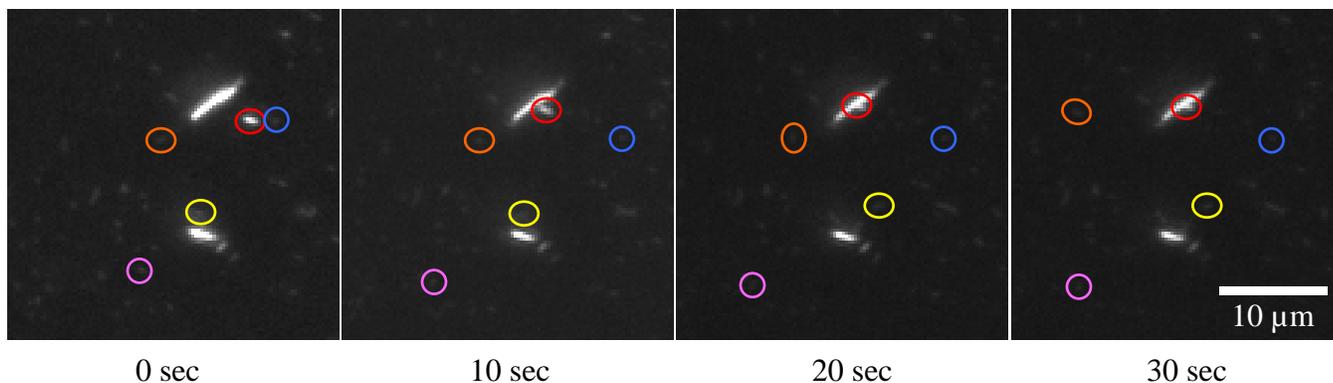

| 0 sec | 10 sec | 20 sec | 30 sec |

Figure 15. Actin motility in a PDMS microfluidic channel. Very small, rhodamine-labeled actin from a solution of actin bundles moves over small distances during a 30 second period of time. PDMS had been plasma treated for 20 minutes to reduce oxygen permeability. The cross-section of the channel was 800 µm x 150 µm.

| 0 sec | 10 sec | 20 sec | 30 sec |
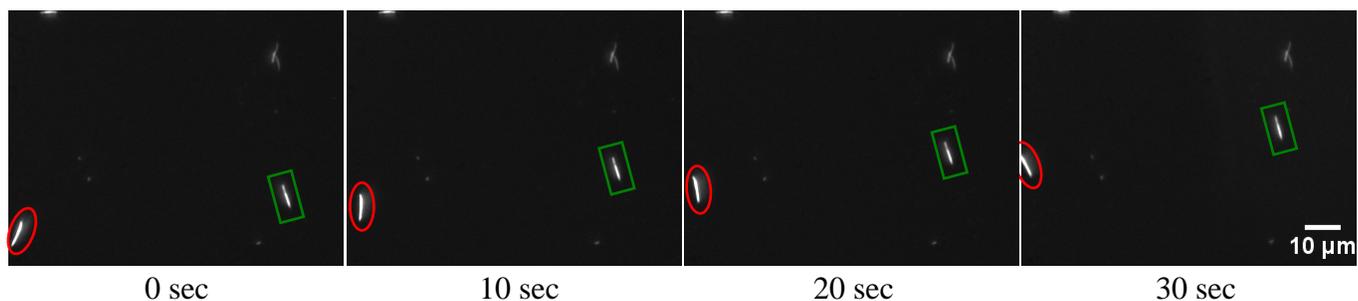
Figure 16. Actin bundle motility in a PDMS microfluidic channel over a period of 30 seconds. The bundles continued to move for longer than 30 seconds but were not tracked. This channel was part of the same device as the channel shown in Figure 15 and was used one day after the device had been constructed.

Reactions at the Surface of a Microfluidic Device (with Laminar Flow)

In our eventual device, HMM motors must be adsorbed to the interior glass surface of the device while laminar flow is occurring in the channel, so we needed to show that protein adsorption and reactions could occur on the device floor under these conditions. It was also convenient to show that these reactions can stay confined to an intersection because intersections

27

could be used to specifically treat certain groups of actin in the future. Patterns created by laminar flow in the device were evident for both the NHS-LC-biotin flow and the neutravidin-FITC flow. This observation suggested that some neutravidin-FITC was nonspecifically bound to the glass, even after blocking with BSA, and also that some contamination of the side channels did occur. However, the most intense fluorescence from the neutravidin-FITC was detected at the intersection (Figure 17), which made the experiment successful by showing that the specific biotin-neutravidin reaction did take place at the surface of the microfluidic device. This result suggests that we should be able to deposit HMM, BSA, and actin onto the surface of our microfluidic device under conditions of laminar flow. Additionally, adding cargo to actin filaments or bundles stopped at an intersection should be able to be achieved using laminar flow. (For additional information regarding the experimental design planned for adding cargo, see Laminar Flow discussion.)
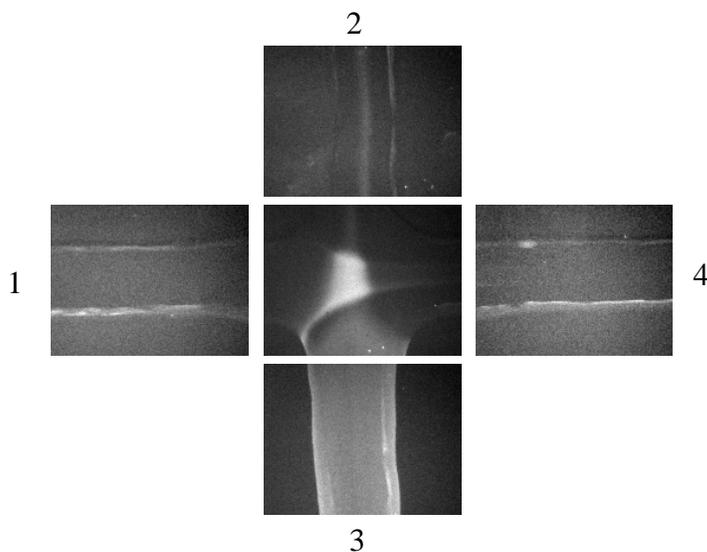

Figure 17. Reaction of NHS-LC-biotin and neutravidin-FITC on the glass surface of a microfluidic device. NHS-LC-Biotin was reacted with a functionalized glass surface in the horizontal channel, and neutravidin-FITC was flowed through the vertical channel. The biotin-neutravidin reaction occurred most strongly at the intersection. See Figure 11 for the experimental setup.

Introducing Actin-Myosin System into Microfluidic Device

When a standard microfluidic device with tubing connections at both ends of the channel is used, many parameters must be optimized. When the proteins in the motility assay are added to a flow cell (or the modified microfluidic device), they are introduced at very specific concentrations and are allowed to incubate with the surface for several minutes. In the standard microfluidic device, reagents are constantly flowing through the channel, which means that the optimal concentrations of reagents used and exposure times at the surface will need to be altered from the standard protocol.

In order to prove that HMM had been deposited in the channel and that actin was bound to myosin and not nonspecifically bound to the channel surfaces, we optimized our conditions for blocking the channels with BSA. Fluorescently-labeled BSA was introduced into microfluidic channels using various flow rates and exposure times. Experiments determined that the channel surfaces were saturated with BSA after 30 minutes of exposure to a 1 mg/mL BSA solution at a flow rate of 0.02 mL/hr. Under these optimized conditions, unlabeled BSA was introduced to a channel, followed by actin. No actin was seen upon imaging, suggesting that BSA was blocking the channel surfaces well. In another channel, HMM was deposited, followed by BSA blocking using the same conditions. After actin was introduced, images showed that actin was bound to the surface, which suggested that we were successful at depositing HMM on the channel surface and binding actin to it.
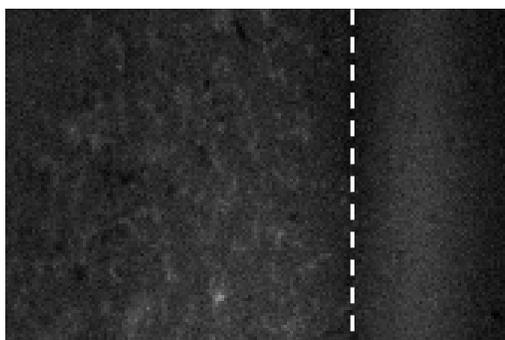
Figure 18. Rhodamine-labeled actin filaments bound to the floor of a microfluidic device. The edge of the microfluidic channel is denoted with the white dashed line. To the left, actin filaments are present inside the channel. To the right, PDMS is bound to the glass to create the channel wall. The device was fabricated using the standard device construction method.

Laminar Flow

One type of flow that can occur in a microfluidic channel is laminar flow, in which individual solutions do not mix, instead forming interfaces within the channel. To further understand this concept and to determine what type of control we had over the flow of solutions within our microfluidic channels, laminar flow experiments were conducted. We were able to determine the conditions necessary to produce laminar flow in a device. Using an optical microscope, we imaged three different colored dye solutions flowing into three inputs of a device (Figure 19). The inputs converged into one common output, where the three colors could be seen exiting the device separate from one another. It was also observed that increasing or decreasing the flow rate of one dye respective to the others could change the total width that the dye occupied within the channel.

Figure 19. Laminar flow in microfluidic channels containing blue (top left), red (bottom left), and green (bottom right) dye solutions. The dyes enter through input channels, meet at the intersection, and display laminar flow in the output channel. Three parallel flows can be seen in the output channel since mixing of the dyes does not occur.

The ability to create laminar flow in our devices enables us to overcome an important obstacle in the design of our device. By using the principle of laminar flow to create a protective sheath flow (buffer-reagent-buffer), we are able to flow reagents past an intersection, as shown in Figure 20. This method should allow us to treat actin bundles stopped in the intersection without contaminating all of the actin in the main channel. The protective sheath flow prevents leakage of reagents into the orthogonal channel at the intersection. In the future, this experimental design will be useful as a means to introduce the reagents necessary to start and stop actin at the intersection and to load or unload cargo.
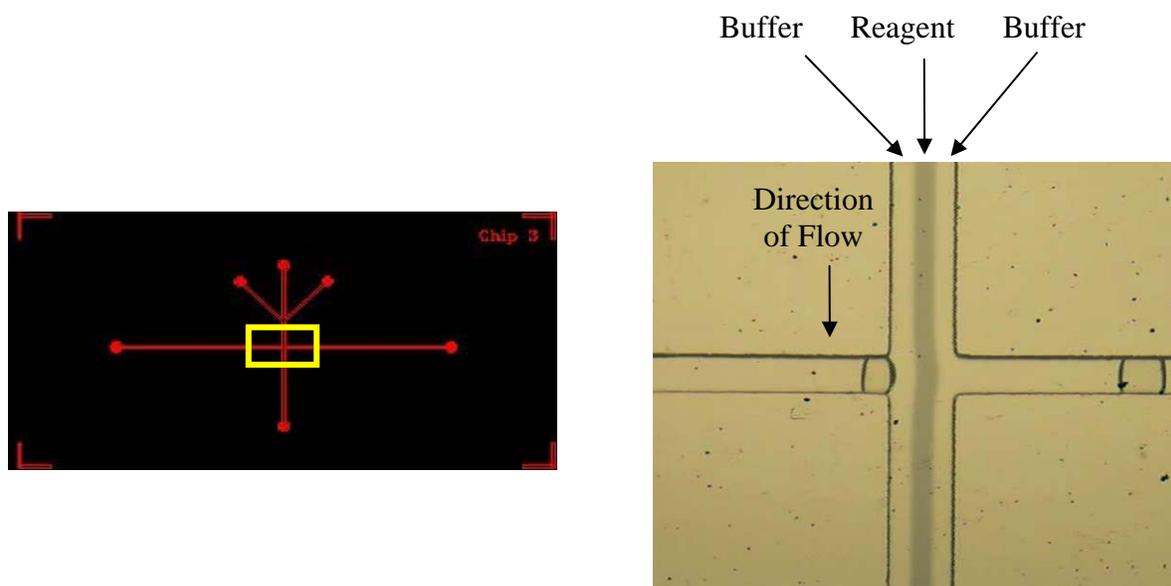
Figure 20. A blue dye solution is flowed past an intersection with the help of a sheath flow of buffer created using the principle of laminar flow. The horizontal channel represents the main channel, containing actin, and the dye solution represents a reagent used to modify the actin. The sheath flow prevents the reagent from contaminating the main channel. Channel widths are 100 µm for the horizontal channel and 200 µm for the vertical channel.

Summary

The incorporation of biomolecular motor systems into microfluidic devices is a very important achievement in the field of nanotechnology, allowing for the creation of nano-cargo transport systems that could be utilized for many different purposes. In this work, we have made a great deal of progress towards incorporating the actin-myosin system into a microfluidic device. Using atomic force microscopy, we showed that a strong cleaning method (piranha solution) achieved a surface with much less variation than one cleaned with water and alcohols. This cleaning technique is important in achieving a good TMS monolayer on the glass after treatment with TMCS. TMCS-functionalized glass surfaces have been shown to work well for use inside of microfluidic devices because solution deposition of the TMCS is easy to perform

inside of the microchannels once they are constructed. We have also demonstrated that PDMS does typically inhibit motility of the actin-myosin system due to its oxygen permeability. However, heavy plasma treatment of the PDMS surface has reduced the permeability enough for motility to be obtained.

Future Work

There is much future work to be done on this project in order to achieve the nano-cargo transport device desired. First, the quality of actin-myosin motility in the PDMS microchannels must be improved so that the actin can travel over the distances and for the lengths of time necessary to transport cargo. Based on our current results, we will attempt to limit the oxygen permeability of the PDMS to a greater extent. A more in-depth study of the plasma treatment conditions required to produce good motility will be done, and other procedures for reducing permeability will be considered. Once consistent motility is obtained in the modified microfluidic device, motility will be attempted in a standard device with the six-port injector and syringe pump. The conditions for flow and solution concentrations will have to be optimized for this system.

Also, once good motility is achieved, a method for starting and stopping the filaments will be employed. We plan to alternate buffer solutions with and without ATP to control the motion of filaments. Eventually, we plan to contain the actin in one main channel, with a perpendicular channel forming an intersection with it. By flowing buffer solutions with and without ATP across the intersection, actin in the intersection will be controlled, allowing eventual loading and unloading of cargo to occur.

Ways to reversibly load and unload cargo onto functionalized actin filaments will also be investigated. A method for functionalizing actin filaments with free thiol groups has already been

33

performed in our lab (Appendix B). This work will be expanded upon in order to attach single-stranded DNA to the actin in a way that motility can still be achieved. This technique will allow cargoes labeled with complementary single-stranded DNA to be attached and carried.

Appendix A

I. Isolation of G-Actin from Acetone Powder/Polymerization of G-Actin to Form F-Actin

1. Weigh out 0.35 g of acetone powder.

2. Add 10 mL of 1 mM $NaHCO_3$ in water for 10 minutes with gentle mixing.

3. Centrifuge for 20 minutes at 4000 rpm and 4°C. Keep supernatant.

4. Repeat step 3.

5. Centrifuge for 1 hour at 40,000 rpm at 4°C. Keep supernatant.

6. Add 1/100 volume of 3M KCl and leave on ice overnight.

7. Centrifuge for 1.5 hours at 40,000 rpm at 4°C. Keep precipitate.

8. Wash pellet with imidazole buffer and remove liquid.

9. Add 200 µL of imidazole buffer and mix heavily to reconstitute pellet.

10. Centrifuge for 15 minutes at 8000 rpm and 4°C. Keep supernatant.

11. Perform Bradford assay to determine protein concentration.

II. Labeling F-Actin with Rhodamine Phalloidin

1. Dry 20 µL of 6.6 µM rhodamine phalloidin using a Speed-Vac (approximately 5 minutes).

2. Add 20 µL of 0.25 mg/mL F-actin and allow the solution to incubate overnight.

III. Bundling F-Actin with Fascin

1. Dilute 1.5 mg/mL fascin with Tris buffer to achieve a 0.625 mg/mL fascin concentration.

2. For a 1:1 (g:g) F-actin: fascin ratio, combine 5 µL of 0.25 mg/mL rhodamine-labeled F-actin, 2 µL of 0.625 mg/mL GST fascin, and 0.6 µL of 0.3 M KCl. (Ratio of F-actin: fascin may have to be altered to achieve suitable bundles.)

IV. Bradford Assay for Determining HMM Concentration

1. Make standard BSA solutions of 0, 200, 400, 600, 800, and 1000 µg/mL by diluting a stock BSA solution of 2 mg/mL with imidazole buffer.

2. Mix 3 µL of each standard with 1 mL of Coomassie blue reagent and vortex. Also, take 2 different 3 µL samples of the HMM solution, mix each with 1 mL of Coomassie blue reagent, and vortex.

3. Pour each standard or sample into a plastic UV-visible cuvette.

4. Using the 0 µg/mL BSA standard as the blank, measure absorbance at 595 nm.

5. Create a standard curve of BSA concentration vs. absorbance.

6. Determine protein concentration of the HMM sample by plotting the experimental absorbance value on the standard curve.

7. Calculate the average concentration of the two HMM samples.

V. Standard Motility Assay

1. Pipette 10 µL of 0.2% collodion in amyl acetate (nitrocellulose) onto a glass coverslip and use pipette tip to evenly spread over the surface.

2. Bake nitrocellulose-coated coverslip at about 75°C for 1 hour.

3. Remove nitrocellulose-coated coverslip from oven and allow to cool for 15 minutes.

4. Construct flow cell by placing two parallel strips of double-sided tape about 0.5 cm apart on a glass slide. Place the nitrocellulose-coated side of the coverslip down on the double-sided tape.

5. Use a pipette tip to add 8 µL of HMM solution to one side of the flow cell. Allow to incubate for 5 minutes.

6. Add 25 µL of 1 mg/mL BSA to the same side of the flow cell used previously. Use a Kimwipe to wick the HMM solution through the opposite end of the flow cell. Allow BSA solution to incubate for 5 minutes.

7. Wash flow cell by adding 25 µL of imidazole buffer and wicking through with a Kimwipe.

8. Add 8 µL of actin solution to flow cell and allow it to incubate for 1 – 5 minutes. (The actin solution is made by diluting the 0.25 mg/mL actin filament stock or the prepared actin bundle stock with imidazole buffer. Dilutions can range from 1/100 to 1/3000

depending on the quality of actin stock and the desired number of filaments/bundles per area. Turning the flow cell upside down so that the nitrocellulose-coated surface is located on the bottom side can help to achieve actin binding, especially if actin bundles are used.)

9. Repeat washing from step 7.

10. Add 18 µL of ATP solution and wick through flow cell. [ATP solution is made with 96:1:1:1:1 imidazole buffer: 150 mM ATP: glucose: glucose oxidase: catalase. DTT (10 mM) and/or methylcellulose (0.3%-0.6%) are sometimes included in the ATP solution.]

11. Image flow cell with a fluorescence microscope to visualize actin motility.

Appendix B: Functionalization of Actin

Procedure

  N-succinimidyl-S-acetylthiopropionate (SATP), hydroxylamine, Ellman's reagent and biotin HPDP were purchased from Thermo Scientific. Actin filaments or bundles were functionalized with thioacetate groups by adding the amine-reactive heterobifunctional crosslinker, SATP (Figure 21-1). 1 mg of SATP was added to 20 µL of DMSO, and this solution was added to 580 µL of imidazole buffer. 3 µL of this solution was then added to the actin filaments and allowed to react for 1 hour on ice. The functionalized actin filaments were placed on dialysis overnight in a refrigerator to remove the excess SATP. The thioacetate groups were converted to thiol groups by addition of 3 µL of 0.5M hydroxylamine (Figure 21-2), and Ellman's reagent was used to determine thiol concentration using UV-visible spectroscopy. Standard motility assay procedures were completed using the functionalized actin filaments to determine the effect of functionalization on motility.
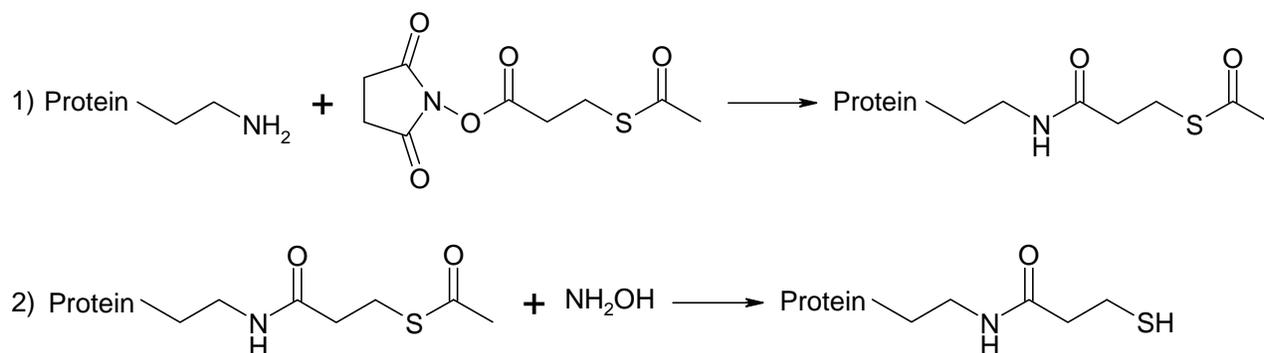

Figure 21. Reactions for functionalizing actin with free thiol groups. In reaction 1, SATP adds a thioacetate group to amine groups on the protein. Hydroxylamine is added in reaction 2, converting the thioacetate group to a free thiol.

Functionalized filaments were also reacted with biotin HPDP and neutravidin-FITC and observed using fluorescence microscopy to determine if the thiol chemistry was working properly. In a separate experiment, fluorescein-labeled, single-stranded DNA with a modified disulfide end was added to functionalized filaments and imaged using an OptiSplit microscope in order to determine if the filaments and DNA were co-localized.

Results and Discussion

We attempted to functionalize the actin with thiol groups in order to create a means for the actin in our device to carry cargo in the future. These thiol groups can be used to perform thiol/disulfide exchange reactions in order to load various cargos. Actin filaments were exposed to SATP, which can add thioacetate groups to lysine residues. The thioacetate groups can later be converted to free thiol groups. After testing various ratios of SATP to NH_2 groups of actin, it was shown that higher relative amounts of SATP caused degradation of the actin filaments (Figure 22). This effect is presumably due to changes in electrostatic forces. The primary amines of the lysine groups present in the actin filaments should have a +1 charge at physiological pH. A neutral charge results when the primary amine groups react with SATP. This change could ultimately affect the protein structure and cause it to lose its native conformation, and therefore lose its functionality. It appears that there is some balance in the number of amine groups that can be functionalized before the actin degrades significantly. Our experiments have shown that a 1:1 ratio of SATP to NH_2 groups is allowable.
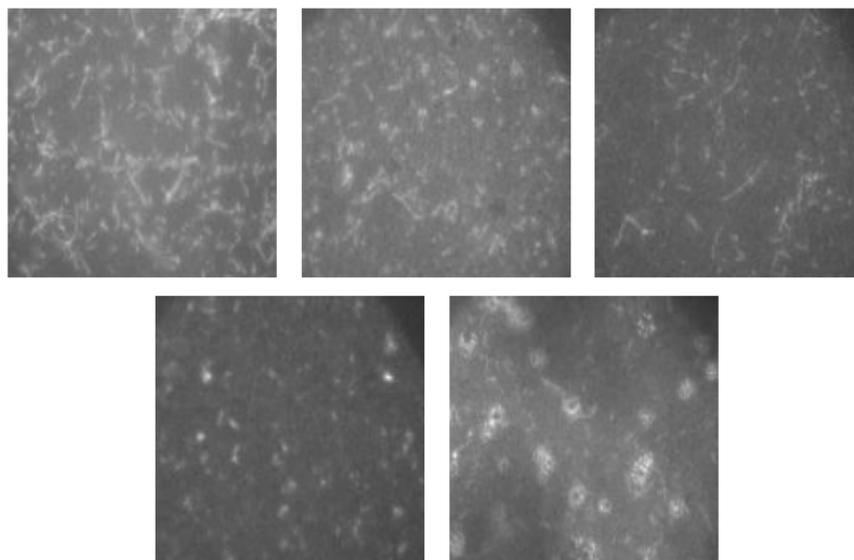
Figure 22. Actin filaments imaged using fluorescence microscopy with the ratio of SATP to NH$_2$ groups increasing from left to right.

Once functionalized actin filaments were obtained, it was necessary to test the motility of the filaments to make sure that they could still be propelled by HMM. Using standard motility procedures, it was observed that motility was obtained with the functionalized filaments after deprotection of the thiol groups (Figure 23).
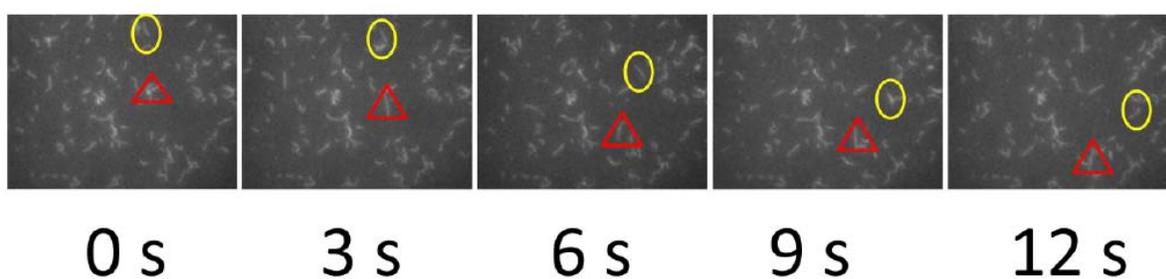

Figure 23. Motility of functionalized actin filaments with free thiols.

We also needed to show that the desired thiol chemistry could be performed. We chose to investigate this question with the commonly used interaction of avidin and biotin molecules. To

test the thiol/disulfide exchange reaction, biotin HPDP (containing a disulfide group) was added to functionalized actin filaments, attaching the biotin molecule to the filament. A neutravidin molecule with a fluorophore attached (neutravidin-FITC) was then introduced to react with the biotin. This setup allowed visualization of the rhodamine filaments superimposed with the fluorescein fluorophore of neutravidin-FITC to show that the chemistry was working properly. However, when this experiment was performed in solution, large aggregations of filaments were seen after the neutravidin-FITC was introduced (Figure 24). It was concluded that this effect was due to neutravidin having four binding sites for biotin. Therefore, each neutravidin-FITC molecule could bind up to four actin filaments, which could also be connected to other filaments via other neutravidin molecules.
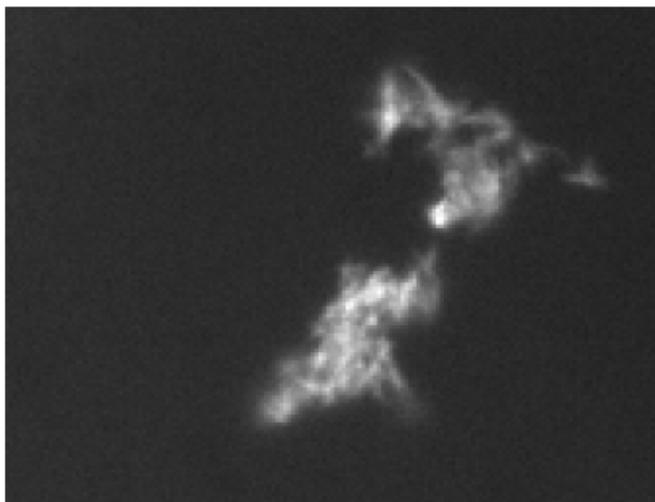

Figure 24. Aggregations of functionalized actin filaments after the addition of neutravidin-FITC.

As a way to carry cargo, we attempted to attach single-stranded DNA to the functionalized actin filaments. Disulfide-modified DNA was used so that a thiol-disulfide exchange reaction would attach the DNA to the actin. Different fluorophores (fluorescein and

rhodamine) were used to label the filaments and the DNA so that they could be detected independently. Using an OptiSplit microscope, both fluorophores could be observed simultaneously so that co-localization of the filaments and DNA could be observed. Superimposable images were obtained (Figure 25), suggesting that DNA did attach to the actin filaments. However, motility has not yet been obtained when DNA is attached, which is potentially due to overloading of the filaments with DNA. Optimization of this attachment still needs to be performed.
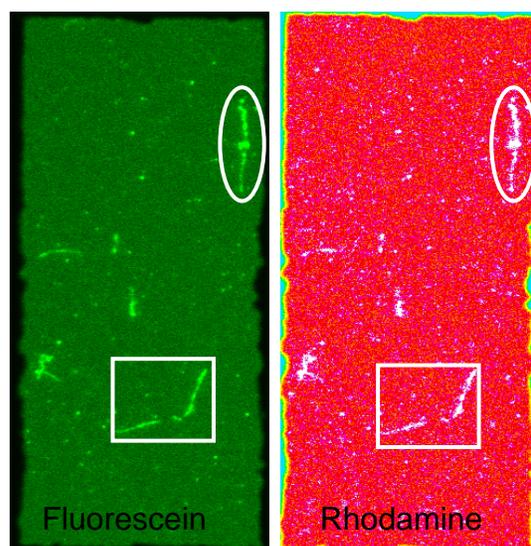
Figure 25. Functionalized actin filaments co-localized with disulfide-modified single-stranded DNA. A 10x excess of fluorescent, single-stranded DNA to thiol group was used. The filaments were imaged using fluorescence microscopy with OptiSplit technology exciting both the fluorescein and rhodamine fluorophores simultaneously. Each channel detects a different fluorophore; therefore overlapping images suggest that both fluorophores are on one filament.

References

1. van den Heuvel, M.G.L.; Dekker, C. Motor proteins at work for nanotechnology. *Science* **2007**, *317*, 333-336.

2. Becker, W.; Kleinsmith, L.; Hardin, J. *The World of the Cell*. (Pearson Education, Inc., San Francisco, ed. 6, 2006).

3. Vale, R.D.; Milligan, R.A. The way things move: Looking under the hood of molecular motor proteins. *Science* **2000**, *288*, 88-95.

4. Geeves, M.A. The dynamics of actin and myosin association and the crossbridge model of muscle contraction. *Biochem J* **1991**, *274*, 1-14.

5. Rayment, I.; Rypniewski, W.R.; Schmidt-Bäse, K.; Smith, R.; Tomchick, D.R.; Benning, M.M.; Winkelmann, D.A.; Wesenberg, G.; Holden, H.M. Three-dimensional structure of myosin subfragment-1: a molecular motor. *Science* **1993**, *261*, 50-58.

6. Voet, D.; Voet, J.G.; Pratt, C.W. *Fundamentals of Biochemistry* 1999 (John Wiley & Sons, Inc.).

7. Steinmetz, M.O.; Stoffler, D.; Hoenger, A. Actin: from cell biology to atomic detail. *J Struct Biol* **1997**, *119*, 295-320.

8. Kron, S.J.; Toyoshima, Y.Y.; Uyeda, T.Q.P.; Spudich, J.A. Assays for actin sliding movement over myosin-coated surfaces. *Method Enzymol* **1991**, *196*, 399-416.

9. Kron, S.; Spudich, J. Fluorescent actin filaments move on myosin fixed to a glass surface. *Proc Natl Acad Sci USA* **1986**, *83*, 6272-6276.

10. Ishikowa, R.; Sakamoto, T.; Ando, T.; Higashi-Fujime, S.; Kohama, K. Polarized actin bundles formed by human fascin-1: their sliding and disassembly on myosin II and myosin V *in vitro*. *J Neurochem* **2003**, *87*, 676-685.

11. Sundberg, M., Rosengren, J. P., Bunk, R., Lindahl, J., Nicholls, I. A., Tågerud, S., Omling, P., Montelius, L., and Månsson, A. Silanized surfaces for in vitro studies of actomyosin function and nanotechnology applications. *Anal Biochem* **2003,** *323* (1): 127-138.

12. Sundberg, M., Balaz, M., Bunk, R., Rosengren-Holmberg, J.P., Montelius, L., Nicholls, I.A., Omling, P., Tågerud, S., and Månsson, A. Selective spatial localization of actomyosin motor function by chemical surface patterning. *Langmuir* **2006**, *22*, 7302-7312.

13. Nicolau, D.V.; Suzuki, H.; Mashiko, S.; Taguchi, T.; Yoshikawa, S. Actin motion on microlithographically functionalized myosin surfaces and tracks. *Biophys J* **1999**, *77*, 1126-1134.

14. Takatsuki, H.; Kolli, M.; Rice, K.M.; Day, B.S.; Asano, S.; Rahman, M.; Zhang, Y.; Ishikowa, R.; Kohama, K.; Blough, E.R. Assembly and function of myosin II on ultraviolet/ozone patterned trimethylchlorosilane substrates. *J Bionanoscience* **2008**, *2*, 1-7.

15. Suzuki, H.; Yamada, A.; Oiwa, K.; Nakayama, H.; Mashiko, S. Control of actin moving trajectory by patterned poly(methylmethacrylate) tracks. *Biophys J* **1997**, *72*, 1997-2001.

16. Hiratsuka, Y.; Tada, T.; Oiwa, K., Kanayama, T.; Uyeda, T.Q.P. Controlling the direction of kinesin-driven microtubule movements along microlithographic tracks. *Biophys J* **2001**, *81*, 1555-1561.

17. Hess, H.; Clemmens, J.; Qin, D.; Howard, J.; Vogel, V. Light-controlled molecular shuttles made from motor proteins carrying cargo on engineered surfaces. *Nano Lett* **2001**, *1*, 235-239.

18. Hess, H.; Matzke, C.M.; Doot, R.K.; Clemmens, J.; Bachand, G.D.; Bunker, B.C.; Vogel, V. Molecular shuttles operating undercover: a new photolithographic approach for the fabrication of structured surfaces supporting directed motility. *Nano Lett* **2003**, *3*, 1651-1655.

19. Moorjani, S.G.; Jia, L.; Jackson, T.N.; Hancock, W.O. Lithographically patterned channels spatially segregate kinesin motor activity and effectively guide microtubule movements. *Nano Lett* **2003**, *3*, 633-637.

20. Clemmens, J.; Hess, H.; Howard, J.; Vogel, V. Analysis of microtubule guidance in open microfabricated channels coated with the motor protein kinesin. *Langmuir* **2003**, *19*, 1738-1744.

21. Huang, Y.; Uppalapati, M.; Hancock, W.O.; Jackson, T. N. Microfabricated capped channels for biomolecular motor-based transport. *IEEE Trans Adv Pack* **2005**, *28*, 564-570.

22. van den Heuvel, M.G.L.; de Graaff, M.P.; Dekker, C. Molecular sorting by electrical steering of microtubules in kinesin-coated channels. *Science* **2006**, *312*, 910-914.

23. Huang, Y.; Uppalapati, M.; Hancock, W.O.; Jackson, T.N. Microtubule transport, concentration and alignment in enclosed microfluidic channels. *Biomed Microdevices* **2007**, *9*, 175-184.

24. Riveline, D.; Ott, A.; Jülicher, F.; Winkelmann, D.A.; Cardoso, O.; Lacapère, J.; Magnúsdóttir, S.; Viovy, J.; Gorre-Talini, L.; Prost, J. Acting on actin: the electric motility assay. *Eur Biophys J* **1998**, *27*, 403-408.

25. van den Heuvel, M.G.L.; Butcher, C.T.; Smeets, R.M.M.; Diez, S.; Dekker, C. High rectifying efficiencies of microtubule motility on kinesin-coated gold nanostructures. *Nano Lett* **2005**, *5*, 1117-1122.

26. Sakamoto, T.; Limouze, J.; Combs, C.A.; Straight, A.F.; Sellers, J.R. Blebbistatin, a myosin II inhibitor, is photoinactivated by blue light. *Biochemistry* **2005**, *44*, 584-588.

27. Takutsuki, H.; Rice, K.M.; Asano, S.; Day, B.S.; Hino, M.; Oiwa, K.; Ishikawa, R.; Hiratsuka, Y.; Uyeda, T.Q.P.; Kohama, K.; Blough, E.R. Utilization of myosin and actin bundles for the transport of molecular cargo. *Small* **2010**, *6*, 452-457.

28. Kovács, M.; Tóth, J.; Hetényi, C.; Málnási-Csizmadia, A.; Sellers, J.R. Mechanism of blebbistatin inhibition of myosin II. *J Biol Chem* **2004**, *279*, 35557-35563.

29. Okuro, K.; Kinbara, K.; Takeda, K.; Inoue, Y.; Ishijima, A.; Aida, T. Adhesion effects of a guanidinium ion appended dendritic "molecular glue" on the ATP-driven sliding motion of actomyosin. *Angew Chem Int Ed* **2010**, *49*, 3030-3033.

30. Nalabotu, S.K.; Takatsuki, H.; Kolli, M.; Frost, L.; Crowder, B.; Yoshiyama, S.; Gadde, M.K.; Kakarla, S.K.; Kohama, K.; Blough, E.R. Control of myosin activity by the reversible alteration of protein structure for applications in the development of a bionano device. *Advanced Science Letters* (in press) **2012**.

31. Månsson, A.; Sundberg, M.; Balaz, M.; Bunk, R.; Nicholls, I.A.; Omling, P.; Tågerud, S.; Montelius, L. In vitro sliding of actin filaments labelled with single quantum dots. *Biochem Bioph Res Co* **2004**, *314*, 529-534.

32. Takatsuki, H.; Tanaka, H.; Rice, K.M.; Kolli, M.B.; Nalabotu, S.K.; Kohama, K.; Famouri, P.; Blough, E.R. Transport of single cells using an actin bundle-myosin bionanomotor transport system. *Nanotechnology* **2011**, *22*, 1-8.

33. Hiyama, S.; Gojo, R.; Shima, T.; Takeuchi, S.; Sutoh, K. Biomolecular-motor-based nano- or microscale particle translocations on DNA microarrays. *Nano Lett* **2009**, *9*, 2407-2413.

34. Schmidt, C.; Vogel, V. Molecular shuttles powered by motor proteins: loading and unloading stations for nanocargo integrated into one device. *Lab Chip* **2010**, *10*, 2195-2198.

35. Hiyama, S.; Moritani, Y.; Gojo, R.; Takeuchi, S.; Sutoh, K. Biomolecular-motor-based autonomous delivery of lipid vesicles as nano- or microscale reactors on a chip. *Lab Chip* **2010**, *10*, 2741-2748.

36. Mukhopadhyay, R. Molecular motors meet microfluidic systems. *Anal Chem* **2005**, *77*, 249A-252A.

37. McDonald, J.C.; Duffy, D.C.; Anderson, J.R.; Chiu, D.T.; Wu, H.; Schueller, O.J.A.; Whitesides, G.M. Fabrication of microfluidic systems in poly(dimethylsiloxane). *Electrophoresis* **2000**, *21*, 27-40.

38. Runge, M.B.; Mwangi, M.T.; Bowden, N.B. New selectivities from old catalysts. Occlusion of Grubbs' catalysts in PDMS to change their reactions. *J Organomet Chem* **2006**, *691*, 5278-5288.

39. Merkel, T.C.; Bondar, V.I.; Nagai, K.; Freeman, B.D.; Pinnau, I. Gas sorption, diffusion, and permeation in poly(dimethylsiloxane). *J Polym Sci Pol Phys* **2000**, *38*, 415-434.

40. Brunner, C.; Ernst, K.-H.; Hess, H.; Vogel, V. Lifetime of biomolecules in polymer-based hybrid nanodevices. *Nanotechnology* **2004**, *15*, S540-S548.

41. Kabir, A.M.R.; Inoue, D.; Kakugo, A.; Kamei, A.; Gong, J.P. Prolongation of the active lifetime of a biomolecular motor for in vitro motility assay by using an inert atmosphere. *Langmuir* **2011**, *27*, 13659-13668.

42. Houston, K.S.; Weinkauf, D.H.; Stewart, F.F. Gas transport characteristics of plasma treated poly(dimethylsiloxane) and polyphosphazene membrane materials. *J Membrane Sci* **2002**, *205*, 103-112.

43. Hillborg, H.; Ankner J.F.; Gedde, U.W.; Smith, G.D.; Yasuda, H.K.; Wikström, K. Crosslinked polydimethylsiloxane exposed to oxygen plasma studied by neutron reflectrometry and other surface specific techniques. *Polymer* **2000**, *41*, 6851-6863.